APPLIED ORGANOMETALLIC CHEMISTRY
Appl. Organometal. Chem. 2001; **15**: 430–434
DOI: 10.1002/aoc.167

Structure and mechanical properties of nanocrystalline boron nitride thin films †

Paolo M. Ossi[1]* and Antonio Miotello[2]
[1]Istituto Nazionale per la Fisica della Materia (INFM) and Dipartimento di Ingegneria Nucleare, Politecnico di Milano, Via Ponzio 34/3, 20133 Milan, Italy
[2]Istituto Nazionale per la Fisica della Materia (INFM) and Dipartimento di Fisica, Università di Trento, Italy

Boron nitride thin films have been deposited on (100) Si wafers, kept at low temperature, by radio frequency (r.f.) magnetron sputtering. The r.f. target power was fixed at 150 W and the substrate bias voltage ranged between −50 and −130 V. Film composition was checked by Auger electron spectroscopy; the structure was investigated by Fourier transform IR spectroscopy, glancing-angle X-ray diffraction and micro-Raman spectroscopy. Film hardness and Young's modulus were measured by nanoindentation. Film composition is nearly equiatomic, with a low degree of gaseous contamination. All samples are very fine grained, and nanocrystalline. Film coordination is mixed sp^2–sp^3, and the fraction of tetrahedral coordination depends critically on the bias voltage value. In hexagonal sp^2-bonded films the hardnesses and Young's moduli are low and increase considerably with the content of sp^3-coordinated cubic phase.

Keywords: solid–solid transitions; thin film structure and morphology; thickness; mechanical and acoustical properties; deposition by sputtering

INTRODUCTION

Boron nitride (BN) is considered one of the most interesting III–V compounds. Among its similarities to carbon, it exists in different allotropic forms,[1] two of which have attracted particular attention: hexagonal, sp^2-bonded BN (hBN) is a soft self-lubricating material, similar to graphite; cubic BN (cBN), with the zincblende structure, is the second hardest material after diamond. Besides being a natural candidate for hard, protective coatings, cBN does not react with ferrous metals, it resists oxidation up to 1573 K, it has a wide band gap ($E_{g,indir} \approx 6$ eV), thus being transparent in the IR and visible regions of the spectrum, it has high thermal conductivity and can be both *p*- and *n*-doped; therefore, it is considered for applications as a high temperature, high-power semiconductor device.

cBN can be prepared as a film, at low pressure, provided a technique involving the bombardment of the growing film with energetic ions is adopted. Among ion-assisted physical vapour deposition (PVD) techniques, radio frequency (r.f.) bias sputtering has been used to deposit BN films. Till now, samples predominantly containing the cubic phase have been obtained only at target powers typically higher than 600 W and at high substrate temperature, above 600 K;[2,3] at low substrate temperature the sp^2-bonded hBN films are obtained.[4] Thus, it is currently true that cBN formation depends critically on three main factors, namely bombardment of the growing film by energetic ions, high substrate temperature and achievement–maintenance of film stoichiometry.

Here we report on both the deposition of cBN thin films by r.f. magnetron sputtering on unheated silicon substrates, at relatively low target power, and on their characterization. The synthesis of films nearly completely cubic at *low* substrate temperature is a basic step towards realistic applications of this material in the microelectronics field.

* Correspondence to: P. M. Ossi, Dipartimento di Ingegneria Nucleare, Politecnico di Milano, Via Ponzio 34/3, 20133 Milan, Italy.
E-mail: paolo.ossi@polimi.it
† Based on work presented at the 1st Workshop of COST 523: Nanomaterials, held 20–22 October 1999, at Frascati, Italy.
Contract/grant sponsor: CNR–Progetto Finalizzato Materiali Speciali per Tecnologie Avanzate II.

Table 1 Collection of deposition parameters and selected properties of BN thin films

Sample number	Sputtering power (W)	Process atmosphere	Bias voltage (V)	Film thickness (nm)	B/N ratio (AES)	cBN/hBN	Nanohardness (GPa)	Young's modulus (GPa)
1	150	$Ar + N_2$	−50	490	1.0	0	2	18.1
2	150	$Ar + N_2$	−70	470	1.1	0.11	7.2	56.3
3	150	$Ar + N_2$	−100	520	1.2	0.97	41.2	285.2
4	150	$Ar + N_2$	−130	500	1.3	0.34	12.3	82

EXPERIMENTAL

BN thin films were deposited on (100) silicon wafers in a vacuum chamber at a base pressure of 1×10^{-5} Pa, using an r.f. target power of 150 W, at −50, −70, −100 and −130 V substrate bias voltages. Besides standard chemical surface cleaning, the substrates were sputter etched in the deposition chamber before starting each deposition. The target material was hBN with nominal purity of 98 at.% and a mixture of 97 at.% argon and 3 at.% nitrogen was chosen as the working gas; during the deposition, the total pressure in the chamber was of 5×10^{-1} Pa. The deposition time was 60 min for all films. Sample temperature, as measured by thermocouples, did not exceed 348 K. Film thickness, as measured by a Dektak profilometer, was around 500 nm.

Chemical characterization of the samples was performed by Auger electron spectroscopy (AES), in a PHI Model 4200 instrument (base pressure in the low 10^{-8} Pa region) equipped with a single-pass cylindrical mirror analyzer with a coaxial electron gun. The electron beam energy and current were 6 keV and 100 nA respectively. Depth profiles were obtained by alternating acquisition and sputtering cycles. Sputtering was performed with 4 keV Ar^+ ions.

To assess the phases of BN films, Fourier transform infra-red (FTIR) spectroscopy was used, because of its high capability to distinguish between sp^3- and sp^2-bonded material. Spectra were taken in dry air, at room temperature, in a differential mode, subtracting the contribution from the silicon substrate, over the spectral range between 500 and 2500 cm^{-1}. The crystal structure was determined by glancing angle (1 °) X-ray diffraction (GXRD) in the Seeman–Bohlin configuration, using Cu Kα radiation. Complementary structural information was obtained by micro-Raman spectroscopy (μ-RS), using a Jobin–Yvon T-64000 spectrometer in the triple subtractive configuration, equipped with a microscope (Olympus BX40) that provides a laser beam diameter of 1 μm at the sample surface. The light source was an Ar^+ laser COHERENT Innova 300, working in single frequency at a wavelength $\lambda = 514.5$ nm, with a spectral resolution of 3 cm^{-1}. Given the high transparency of BN in the visible and the low Raman cross-section of cBN, the output power was fixed at 200 mW, the power at sample surface being 50 mW. Also, a BN film was deposited at −100 V substrate bias voltage onto a (100)Si substrate uniformly coated with 600 nm of titanium. This allows one to avoid the spectral contribution from the TO second-order peak of silicon at 970 cm^{-1}, which largely overlaps with the comparatively weak peak at 1056 cm^{-1} from cBN. All spectra were recorded at room temperature, over the wavenumber interval 600–1600 cm^{-1}. Mechanical properties were tested with a NanoInstruments (type II), ultra-low load depth-sensing nanoindenter, in constant displacement rate mode, up to a total depth of 50 nm. Details of the procedure are reported elsewhere.[5]

RESULTS AND DISCUSSION

Table 1 reports the deposition conditions and results of different analyses for the films studied.

The B/N atomic composition ratio, which is a parameter strongly affecting cBN nucleation, lies between 1.0 and 1.3, as deduced from an analysis of the KVV Auger transitions at 179 eV (B) and 379 eV (N). Owing to partial charging of the insulating bulk BN standard during electron irradiation, depth profiles are to be taken as semi-quantitative analyses, based on the use of literature sensitivity factors.

From typical spectra for hBN (Fig. 1a, sample 1) and for cBN (Fig. 1b, sample 3), carbon contamination is present only in the near-surface region, while oxygen extends across the whole film thickness in concentrations not higher than 10

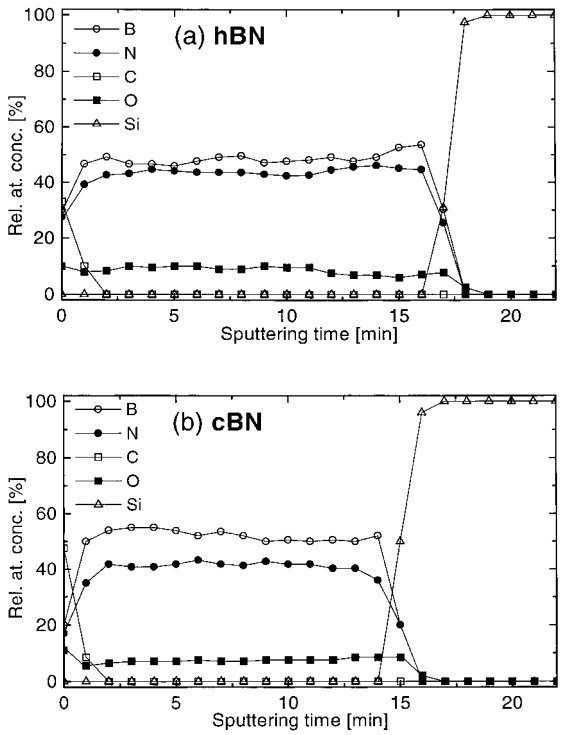

Figure 1 AES depth profiles of representative hBN (a) and cBN (b) films.

at.% (hBN) and 7 at.% (cBN). Figure 2 shows the FTIR absorption spectra of sample 1 (Fig. 2a) and of sample 3 (Fig. 2b). Two absorption bands, peaked at 1335 and at 766 cm^{-1}, are evident in the spectrum of sample 1; these correspond to the in-plane stretching B—N mode at 1370 cm^{-1} and to the B—N—B out-of-plane bending mode at 783 cm^{-1} of bulk hBN.[6] The spectrum of sample 3 displays an intense absorption band at about 1107 cm^{-1}, which is associated with the TO mode of cBN (1065 cm^{-1} in bulk cBN[7]); also visible in the spectrum are weak contributions from sp^2-bonded material, centered around 775 and 1378 cm^{-1}. The fraction of cubic phase is given by the intensity ratio $I_c/(I_c + I_h)$, where the subscript h refers to the stretching mode in the hexagonal phase. Data were fitted using Lorentzian peak functions to determine each integrated peak intensity.[8] Although commonly adopted in the analysis of spectra recorded in transmission geometry, the quantification procedure based on film absorbance may lead to an overestimate of the cBN content in mixed-phase films. In our samples, the linear approximation of the Lambert–Beer law is verified and we made use of the correlation between the ratio of absorption coefficients α (1065 cm^{-1})/α(1370 cm^{-1}) and the ratio of volume fractions f_{cBN}/f_{hBN}.[9] The cBN fractions reported in Table 1 were determined in this way.

The residual stress in cBN films was estimated by comparing the shift of the IR band maximum[2] with respect to the literature value[7] in a delaminated cBN film, in which stresses were almost completely released, and the corresponding shift in a well-adherent cBN film. A stress of about 5 GPa was found in the delaminated sample, whereas in the adherent film the calculated residual stress was as high as 19 GPa. This value is an upper limit, because the shift of the IR band maximum can also be influenced by film thickness and crystallinity degree (see XRD analysis below).

Figure 3 shows the GXRD spectra of samples 1 and 3; in the spectrum of sample 1 the hBN (100)

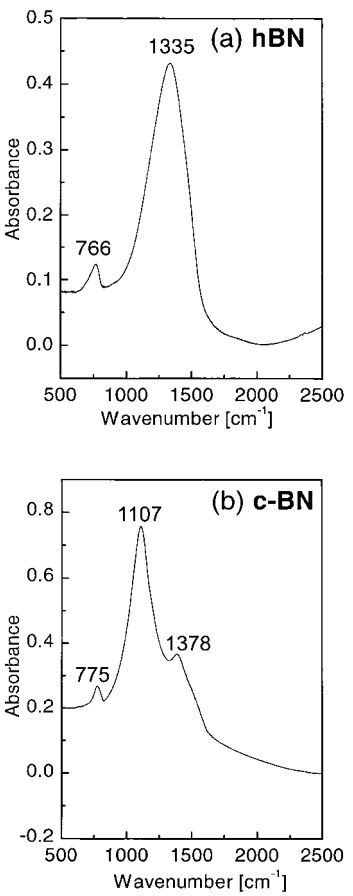

Figure 2 Typical FTIR spectra of representative hBN (a) and cBN (b) films. Band maxima are indicated.

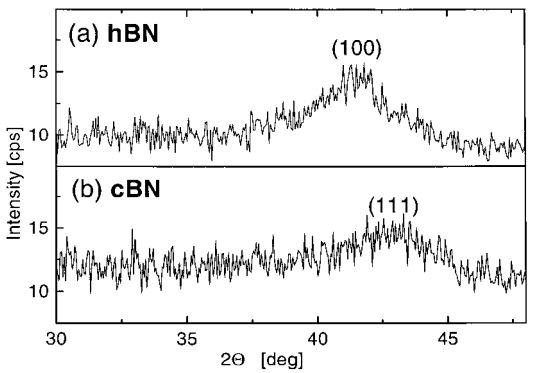

Figure 3 GXRD patterns of representative hBN (a) and cBN (b) films. Peak maxima are indicated.

peak at 41 °47′ (literature value[10] 41 °60′) is found and in the spectrum of sample 3 only the cBN (111) peak at 43 °25′ (literature value[11] 43 °30′) is present. Such a finding agrees with the observed preferential (111) orientation of cBN films grown under ion-assisted processes.[12] As to the X-ray pattern of hBN, the absence of the (002) peak at 26 °80′ coincides with the observation[13] that in sp^2-bonded material grown under ion bombardment the (002) planes are preferentially oriented normal to the substrate. Stress can affect both the X-ray peak position and the width; in the more critical case of cBN, given a Young's modulus around 285 GPa (see Table 1), a compressive stress in region the of 10 GPa could result in a shift of the (111) peak by about 2 ° towards higher angular positions; the practically unaltered peak position with respect to the literature value indicates that film internal stress, as evaluated from IR data, is presumably overestimated. In polycrystalline samples the peak broadening is related to both grain size and lattice distortion; the effect may be relevant in nanocrystalline layers with elevated internal stresses. The strain contribution to the broadening of a peak centered at 2θ is given[14] by $4 \tan^2 \theta <e^2>$, where $e = (\Delta d/d)$ is the local strain. Assuming the high internal stress value estimated by the IR peak shift, the strain contribution to the full-width at half maximum (FWHM) of the peak at 43 °25′ is still one order of magnitude lower than the measured one. From a Scherrer analysis of grain-size-induced FWHM of the Bragg peaks, a correlation length ξ of 1.5 nm was deduced for cBN. In hBN, the interplanar ξ value is 1.6 nm; the corresponding intraplanar value[15] is 3.2 nm.

Figure 4a and b shows the Raman spectra of an hBN (sample 1) and of a cBN film (sample 3)

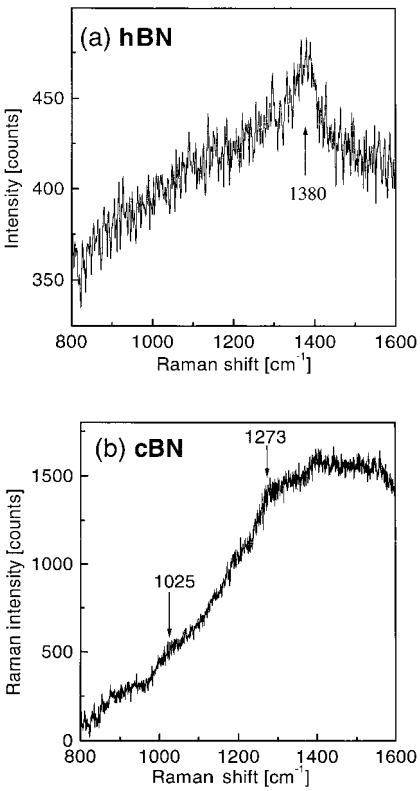

Figure 4 μ-RS of representative hBN (a) and cBN (b) films. The relevant features are indicated.

respectively; in both of them the arrows mark the positions of the relevant features. As a rule, both spectra were fitted with two Gaussians, without imposing maxima positions. Corresponding to the high wavenumber E_{2g} phonon mode of hBN, a peak centered at 1380 cm^{-1}, with an FWHM of 62.4 cm^{-1} (Fig. 4a), is observed. With the literature value[15] of 1366 cm^{-1}, adopting the intraplanar ξ value of 3.2 nm from X-ray data, and using the relation for a confinement-induced peak shift in hBN,[12] a peak shift to 1380 cm^{-1} with FWHM of 52.4 cm^{-1} is obtained, in agreement with the Raman data.

cBN single crystals display two Raman active modes,[16] at 1056 cm^{-1} (TO) and 1306 cm^{-1} (LO). Raman spectra of cBN thin films have been rarely studied owing to the very low light absorption of the material caused by the wide band gap. Peak visibility is further lowered in films due to phonon confinement, associated with small crystal size and high defect density. In nanocrystalline films, the TO and LO peaks degrade into a single, broad and rather unstructured phonon band (see Fig. 4b). Thus

the Raman spectra of cBN films cannot give, at present, independent structural indications owing to the extreme signal weakness.[17] In Fig. 4b, two weak features, as obtained by curve fitting, are marked at 1025 and 1273 cm^{-1}. Taking into account the reported size-induced red shift of the TO phonon peak in cBN single crystals,[17] a shift from 1056 to 1025 cm^{-1} is found. The LO peak maximum correspondingly shifts from 1306 to 1280 cm^{-1}. Notice that such an agreement with experiment should be taken with care, given the overall signal weakness. We observe that the X-ray-determined correlation length is attributed exclusively to grain-size effects, yet the same degree of phonon confinement could equally result from a microstructure including larger grain sizes, in the presence of defects such as vacancies, interstitials, and foreign atoms, mainly oxygen and argon. Argon originates from the process atmosphere and oxygen is incorporated accidentally during film growth, given the base pressure value (10^{-5} Pa). The combined effect of a low Raman cross-section, a high defect density and small grain size is responsible for the very low intensity of Raman signals.

Owing to the potential uses of cBN, the mechanical properties of films deposited with different process conditions were investigated and a range of hardness and elastic modulus values were reported.[4] As a rule, these are markedly lower than those of cBN single crystals. The considerable data scattering is attributed to the difficulty of the measurements in, usually, thin films, so that shallow indentation depths, less than 50 nm, are to be adopted. If surface roughness is meaningful, measurements are not reliable, besides being influenced by elastic and plastic contributions from the substrate.

Nanoindentation measurements have been possible on all our films, owing to their considerable thickness; hardness values and Young's moduli (see Table 1) agree with the assignment of crystalline structure to the different films: the values increase progressively with increasing content of sp^3-bonded material, from values typical of soft hBN[18] to values approaching the upper limit of the range reported for films containing a large fraction of cubic phase.[4]

In conclusion, the attainment at a temperature not higher than 348 K of predominantly cubic-phase BN films was possible. The influence of the bias voltage applied to the substrate on cBN abundance was explored and a critical dependence of film structure on bias voltage was observed; this could support the subplantation model.[19] The role of substrate temperature on cBN formation is certainly questioned by our results. Structural analysis indicates that the films are polycrystalline, with grain size in the nanometric range, thus giving rise to strong phonon confinement effects.

Acknowledgements The authors are grateful to R. Checchetto and G. F. Menestrina (University of Trento) for film deposition and for providing the FTIR apparatus, T. Sasaki (JRC Ispra) for nanoindentation measurements, A. Mantegazza (Politecnico di Milano) for technical assistance with Raman spectroscopy, and C. E. Bottani (Politecnico di Milano) for valuable discussion on Raman analysis.

Financial support by CNR–*Progetto Finalizzato Materiali Speciali per Tecnologie Avanzate II* is acknowledged.

REFERENCES

1. Medlin DL, Friedman TA, Mirkarimi PB, Mills MJ, McCarty KF. *Phys. Rev. B* 1993; **50**: 7884.
2. Ulrich S, Sherer J, Schawan J, Barzen I, Jung K, Scheib M, Ehrhardt H. *Appl. Phys. Lett.* 1996; **68**: 909.
3. Hahn J, Richter F, Pintaske R, Roeder M, Schneider E, Welzel T. *Surf. Coat. Technol.* 1997; **92**: 129.
4. Mirkarimi PB, McCarty KF, Medlin DL. *Mater. Sci. Eng. R* 1997; **21**: 47.
5. Beghi MG, Bottani CE, Miotello A, Ossi PM. *Thin Solid Films* 1997; **308–309**: 107.
6. Geick R, Penny CH, Rupprecht G. *Phys. Rev.* 1966; **146**: 543.
7. Gielisse PJ, Mitra SS, Plendl JN, Griffis RD, Mansur LC, Marshall R, Pascoe EA. *Phys. Rev.* 1967; **155**: 1039.
8. Klett A, Freudenstein R, Plass MF, Kulish W. *Surf. Coat. Technol.* 2000; **125**: 190.
9. Jäger S, Bewilogua K, Klages C-P. *Thin Solid Films* 1994; **245**: 50.
10. Powder Diffraction File Sets 1-42, ICCD 1992, 34–421.
11. Powder Diffraction File Sets 1-42, ICCD 1992, 35–1365.
12. Murakawa M, Watanabe S, Miyake S. *Diam. Films Technol.* 1991; **1**: 55.
13. Kester DJ, Ailey KS, Davis RF, Moore KL. *J. Mater. Res.* 1993; **8**: 1213.
14. Klug HP, Alexander LE. *X-Ray Diffraction Procedures for Polycrystalline and Amorphous Materials*. John Wiley and Sons: New York, 1974; 660.
15. Nemanich RJ, Solin SA, Martin RM. *Phys. Rev. B* 1981; **23**: 6348.
16. Eremets MI, Gauthier M, Polian A, Chervin JC, Besson JM, Dubitskii GA, Semenova YY. *Phys. Rev. B* 1995; **52**: 8854.
17. Werninghaus T, Hahn J, Richter F, Zahn DRT. *Appl. Phys. Lett.* 1997; **70**: 958.
18. Gissler W, Haupt J, Crabb TA, Gibson PN, Rickerby DG. *Mater. Sci. Eng. A* 1991; **139**: 284.
19. Lifshitz Y, Kasi SR, Rabalais JW, Eckstein W. *Phys. Rev. B* 1990; **41**: 10 460.

